Dual-Band MIMO Antenna with Four CPW Elements using Polarization Diversity for 5G Mobile Communication Networks and Satellite

Doae El Hadri[1], Asmaa Zugari[2], Alia Zakriti[1] and Mohssine El Ouahabi[1]

[1]Laboratory of Sciences and Advanced Technology, Department of Civil and Industrial Sciences and Technologies, National School of Applied Sciences, Abdelmalek Essaâdi University, Tetuan, Morocco

[2]Information and Telecommunication system Laboratory, Faculty of Sciences, Abdelmalek Essaâdi University, Tetuan, Morocco

Corresponding author: Doae El Hadri (e-mail: doae93@gmail.com).

ABSTRACT In this paper, a novel design of compact quad-element MIMO (Multiple Input Multiple Output) antenna for 5G communication networks and satellites is proposed. The four similar elements of this antenna are placed perpendicularly to each other on a 40x40 mm^2 FR4 substrate. Each element is fed by a CPW (coplanar waveguide) line. Two slits and an I-shaped slot are etched into the patch, and by varying their parameters; a good matching is achieved in the lower (4.9 GHz) and upper (17 GHz) frequency bands. However, 25 and 30 dB isolations are attained in the lower and upper bands, using the polarization diversity technique and adding stubs on the ground plane. A prototype of the proposed antenna is fabricated and measured. Moreover, the performance of the MIMO antenna is studied in terms of ECC (envelope correlation coefficient), DG (diversity gain), TARC (total active reflection coefficient), realized gain, efficiency, and radiation pattern, validated with the measured results, and showed a good agreement.

INDEX TERMS CPW dual-band antenna, 4x4 MIMO antenna, inserting stub, polarization diversity, fifth generation.

I. INTRODUCTION

A rapid development of wireless communication technologies has been observed. The data rate is the main characteristic that differentiates the different generations (from 1G to 5G) of wireless technology, which is increasing progressively. Indeed, the fifth-generation 5G mobile communications network will deliver a high data rate of 10 Gbps or more [1].

To meet the demand for high-throughput, MIMO (multi-input multi-output) technology is considered one of the fifth-generation core networks. It uses multiple antennas for transmitting and receiving signals in wireless communications. This technology improves multipath propagation and channel capacity without increasing transmission power. In addition, it is used to increase SNR, and data rate, improve the Quality of Service (QoS), enhance coverage, and provide better spectral efficiency [2]. It is worth noting that increasing the number of antenna elements at the transmitter and the receiver ends results in a significant upgrade in data rate and channel capacity [3].

One of the critical factors that must be considered in the design process is the compactness of the antenna. On the other hand, there is strong mutual coupling when the distance between MIMO antennas is very close. Above all, we know that mobile terminals have limited space. To overcome this drawback, the isolation between the radiating elements must be very high. This necessitates the application of the decoupling technique. Therefore, the major challenge for designers and researchers is to strike a balance between miniaturization and high isolation.

In this context, in the literature, there are different techniques such as spatial diversity [4], polarization diversity [5-7], neutralizing line [8-11], T-shaped parasitic structure [12], slots [1], Metamaterial [13], Defected Ground Structure (DGS) [14], split-ring resonators (SRR) [15, 16] are used to enhance isolation. [17] presents a detailed study of the various isolation enhancement techniques.

The allocation of spectrum is one of the main concerns of 5G mobile communications. The fifth generation 5G technology utilizes a different frequency spectrum and can operate in two frequency categories. The first category (lower spectrum) called “sub 6 GHz” covers frequencies such as: 5G NR bands N77 (3.3 GHz-4.2 GHz), N78 (3.3 GHz-3.8 GHz) and N79 (4.4 GHz-5 GHz) [18, 19]. The second category (higher frequency) is called millimeter waves, like 28 GHz (27.5 - 28.35), 37 GHz (37 - 38.6), 39 GHz (38.6 - 40), and frequency band 64 - 71 GHz allocated by FCC [20].

Furthermore, multiband antennas are a fascinating topic as their advantage is reducing the number of antennas on board

by combining several applications on the same antenna and allowing simultaneous coverage of different bands.

This work proposes a novel compact dual-band quad-element MIMO antenna for the 5G communication networks and satellites. The suggested CPW MIMO antenna consists of four radiating elements placed orthogonal to each other using the polarization diversity technique. A detailed study, from the single-element CPW antenna to four-element MIMO antenna is presented. Performance metrics of the MIMO antenna in terms of envelope correlation coefficient (ECC), diversity gain (DG), total active reflection coefficient (TARC), realized gain, radiation efficiency, and radiation pattern are evaluated. A prototype of the proposed single and MIMO antenna has been fabricated and measured, and a good agreement between simulations and measurement results has been obtained. The benefits and the novelties of the proposed antenna can be described as follows:

Simplicity: A simple structure is designed and fabricated using a low-cost FR4 substrate. Therefore, the structure can be easily included in practical applications.

Feeding Technique: A CPW line feeds the proposed antenna. This line presents a flexibility of design and realization; it also shows a facility of integration with other circuits thanks to its uniplanar character.

Compact size: The proposed MIMO antenna is fabricated in a small size of (40x40 mm^2), which realizes the miniaturization.

Stable radiation patterns: The antenna has bidirectional radiation in the E-plane and omnidirectional radiation in the H-plane. This kind of stable radiation pattern is preferred in modern wireless applications.

Radiation efficiency: The radiation efficiency of the proposed antenna is 70% and 65% at lower and upper-frequency bands, respectively.

Good impedance matching: The values of |S11| are 29.99 and 30.26 for the desired bands, which means a better impedance matching at the two bands.

Diversity performance: The proposed antenna has high isolation and low correlation in the two operating bands, which make the proposed antenna a good candidate for MIMO applications.

Novelty: The proposed antenna can support dual-band operation corresponding to 5G and satellite applications with excellent MIMO characteristics, thanks to the polarization diversity and the use of slots and stubs.

II. Antenna design and analysis

A. SINGLE CPW DUAL-BAND ANTENNA

Coplanar waveguide (CPW) consists of a center strip conductor with a pair of ground planes on either side separated by a small gap g, as demonstrate in Fig. 1(b). Fig. 1 illustrates the geometry of the proposed CPW dual-band antenna with detailed dimensions. The suggested antenna is fed by a 50 Ohm characteristic impedance CPW line. The proposed antenna is fabricated on an FR4 substrate with a relative permittivity of 4.4, a thickness of 1.6 mm and a loss tangent of 0.02. The overall size of the CPW dual-band antenna is 20x20 mm^2. The antenna is composed of two slits etched on the left and right side of the radiating element, an I-shaped slot, and a rectangular stub inserted in one pair of the ground plane. The antenna is designed and simulated using Computer Simulation Technology (CST) Microwave Studio Software.

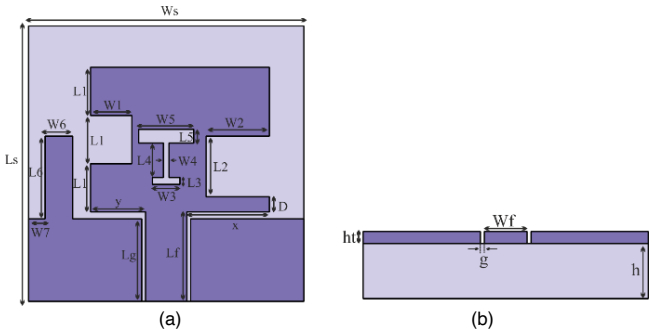

FIGURE 1. Geometry of the proposed CPW dual band antenna (a) top view (b) side view.

B. FOUR-PORT CPW DUAL-BAND MIMO ANTENNA

Based on a single CPW dual-band antenna, a 4x4 MIMO antenna array has been designed with substrate dimensions of 40x40x1.6 mm^3. The optimized dimensions of the proposed CPW dual-band MIMO antenna are shown in Table 1. The proposed CPW dual-band MIMO antenna consists of four symmetrical element antennas arranged perpendicularly to each other, as shown in Fig. 2.

TABLE I. OPTIMIZED DIMENSIONS OF THE PROPOSED MIMO ANTENNA

Parameter	WS	LS	h	ht	WF	LF	g	Lg	W
Value(mm)	20	20	1.6	0.035	3	6.5	0.28	6	40
Parameter	x	y	W1	D	L2	W2	L1	W5	L
Value(mm)	6	4	3	1.1	4.4	4.6	3.5	4	40
Parameter	L5	L4	W4	W3	L3	W7	L6	W6	S
Value(mm)	1	2.5	0.4	2	0.5	1.2	6	2	5.5

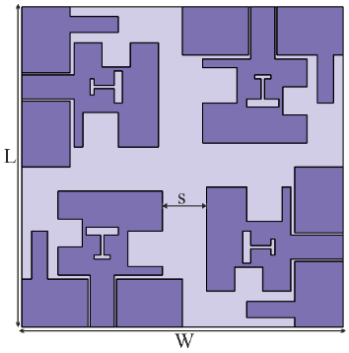

FIGURE 2. The geometry of the proposed 4x4 MIMO antenna.

C. DESIGN EVOLUTION

The CPW dual-band antenna design steps and the corresponding reflection coefficients are shown in Figs. 3 and

4, respectively. A step-by-step description of each of these stages is described below:

Firstly, we start with a conventional CPW antenna (Antenna 1). The reflection coefficient corresponding to this antenna is represented in Fig. 4. From this figure, the operating frequency is 17 GHz for the upper-frequency band and about 6 GHz for the lower-frequency band.

Secondly, to shift the resonant frequency from 6 GHz to 4.9 GHz, two slits are etched at the left and the right of the radiating element (Antenna 2). As can be seen from Fig. 4, the lower-frequency band is 4.9 GHz with S_{11}=-15 dB, while the upper-frequency band is 17 GHz with S_{11}=-25 dB.

Thirdly, an I-shaped slot is etched into the patch (Antenna 3), to adapt the upper-frequency band. As shown in figure 4, the reflection coefficient is adapted from -25 dB to -42 dB.

Finally, to adapt the lower-frequency band, a stub is inserted on the left ground plane (Antenna 4). From figure 4, the reflection coefficient curve corresponding to (Antenna 4) shows that the two desired frequency bands (4.9 GHz and 17 GHz) are well matching.

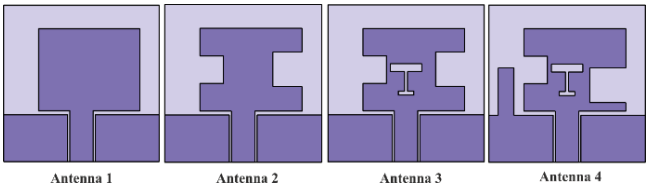

FIGURE 3. The evolution of the proposed CPW dual-band antenna.

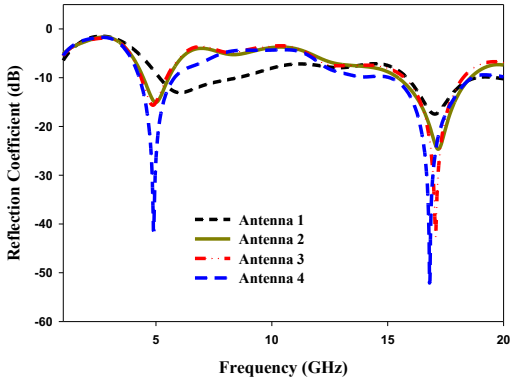

FIGURE 4. Reflection coefficient of all antennas.

D. PARAMETRIC STUDY

The purpose of this section is to study the effect of antenna parameters on frequencies and adaptation. The parametric study was carried out using Computer Simulation Technology (CST) Microwave Studio software. This parametric study aims to achieve optimal values and good performance by adjusting only one parameter and keeping the other parameters constant.

1) EFFECT OF "W1, D, L2, AND W2" PARAMETERS OF SLITS

Two slits are etched on the radiating element; the slit etched on the left has the length L1 and width W1, while the slit etched on the right at a distance D from the feed line has the length L2 and the width W2. Fig. 5 represents the effects of W1, D, L2 and W2 parameters on the reflection coefficient of the proposed CPW dual-band antenna.

Fig. 5 (a) shows the simulated reflection coefficient when W1 changed from 2.5 mm to 3 mm. We can observe that when W1 increases, the first frequency band shift towards the lower frequencies, it is clear that this slit is the responsible for that band. The optimal value is chosen to be W1=3 mm.

Fig. 5 (b) presents the simulation of the reflection coefficient for various values of D. When the value of D decreases from 4.1 mm to 1.1 mm with a step of 1mm, the second frequency shifts to the high frequency with a good impedance matching, D=1.1 mm is the optimal value.

The effect of the length L2 on the reflection coefficient is indicated in Fig. 5 (c); according to this figure, we notice that there is not a significant effect on the two bands, but for the upper band, we can see that for L2=4.4 mm a good adaptation is obtained in comparing to the other values of L2, this is why the optimal value of L2 is 4.4 mm.

Fig. 5 (d) illustrates the simulated reflection coefficient versus frequency with different values of W2. From this figure, we remark that the variation of the width W2 from 4 mm to 4.6 mm shifts the first band to the lower frequencies and adapts the second band. Since our objective is to obtain a resonant frequency of 4.9 GHz, the optimal value is, therefore, W2=4.6 mm.

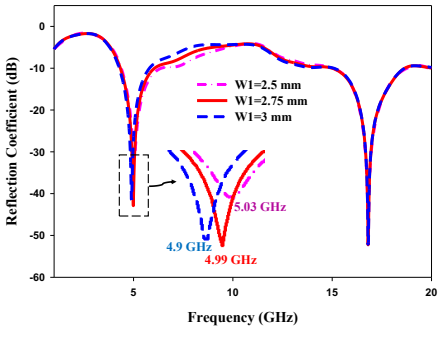

(a)

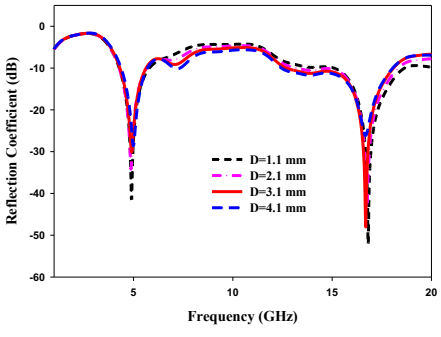

(b)

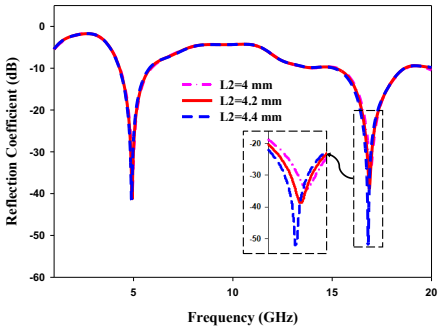

(c)

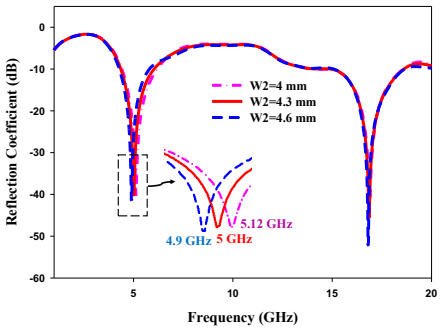

(d)

FIGURE 5. Simulated S_{11} parameter for different values of: (a) W1, (b) D, (c) L2 and (d) W2.

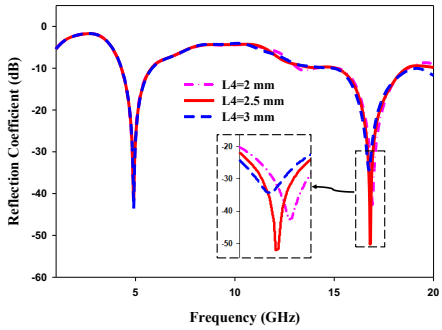

(a)

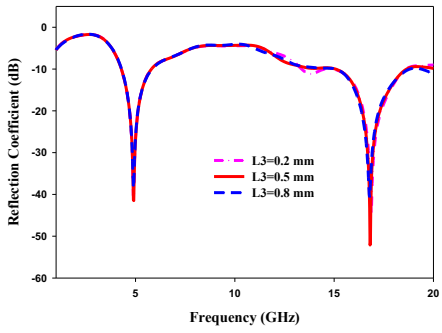

(b)

FIGURE 6. Simulated S_{11} parameter for different values of: (a) L4 and (b) L3.

2) EFFECT OF "L4, L3" PARAMETERS OF I-SHAPED SLOT

An I-shaped slot is introduced into the patch to improve impedance matching at the upper-frequency band (17 GHz). This slot has the dimensions of W3=2 mm, L3= 0.5 mm, W4=0.4 mm, L4= 2.5 mm, W5=4 mm and L5=1 mm.

Fig. 6 (a) illustrates the simulated S_{11} parameter for different values of L4. It is clear from this figure that the variation of the L4 parameter affects the upper band, but the lower frequency band remains unchanged. The results show that the reflection coefficient corresponding to the desired frequency band is good for L4=2.5 mm.

The curve of the simulated reflection coefficient for different values of the L3 parameter is shown in Fig. 6 (b). It is evident from this figure that changing the value of the length L3 affects the adaptation of the upper-frequency band. The optimal value is L3=0.5 mm.

3) EFFECT OF "L6, W6" PARAMETERS OF STUB

To adapt the frequency bands, a stub is inserted at the left ground plane with a distance of W7=1.2 mm from the left edge of the substrate. The width stub is W6, and its length is L6.

The L6 parameter plays a crucial role in adapting the lower frequency band. Fig. 7 (a) shows the reflection coefficient for different values of L6. From this figure, it is clear that for L6=6 mm, good impedance matching is achieved, which is why the optimal value is L6=6 mm.

Fig. 7 (b) illustrates the reflection coefficient for various values of W6. By changing the W6 parameter from 1 mm to 2 mm with a step of 0.5 mm, a good adaptation is noticeable in the upper-frequency band. To make the antenna achieve the best performance, the optimal value is W6= 2 mm.

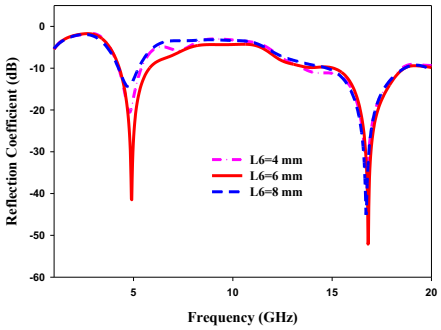

(a)

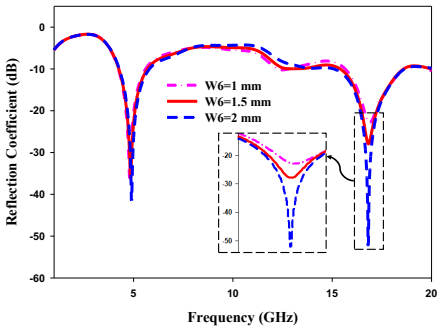

(b)

FIGURE 7. Simulated S_{11} parameter for different values of: (a) L6 and (b) W6.

This parametric study illustrates the simulated reflection coefficient of the proposed CPW dual-band antenna with optimal dimensions in Fig. 8.

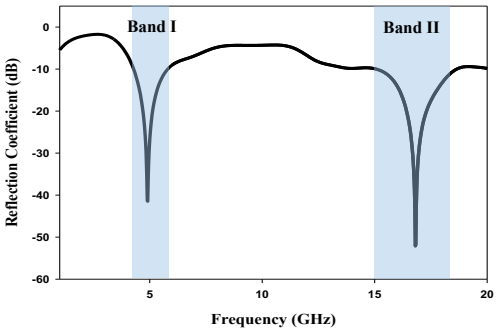

FIGURE 8. Simulated S_{11} parameter of the proposed single CPW dual-band antenna.

From Fig. 8, the reflection coefficient S_{11} is adapted with -42 dB at the lower-frequency band (4.9 GHz) and -52 dB at the upper-frequency band (17 GHz). The impedance bandwidths are [4.28-5.7 GHz] and [15-18.6 GHz], covering 5G and satellite bands, respectively.

E. MUTUAL COUPLING

Once the CPW dual-band antenna has been completed, the arrangement of the four elements of this antenna will be made using the polarization diversity technique to obtain the desired 4x4 MIMO antenna array.

As shown in detail above, the stub inserted in the left ground plane, which adapts the lower frequency band, also effects the isolation, which will be demonstrated in the following paragraph.

Fig. 9 shows the S-parameters of the CPW dual-band MIMO antenna without and with stub. Due to the symmetry $S_{11}=S_{22}=S_{33}=S_{44}$, $S_{21}=S_{32}=S_{43}=S_{14}$, $S_{31}=S_{42}=S_{13}=S_{24}$, and $S_{41}=S_{12}=S_{23}=S_{34}$, we will only be interested in the analysis of S_{11}, S_{21}, S_{31}, and S_{41} parameters. Table 2 summarizes the values of the reflection and transmission coefficients of the MIMO antenna for the two frequency bands.

TABLE II. S-parameters of 4x4 MIMO antenna without and with stub

		$\|S_{11}\|$ (dB)	$\|S_{21}\|$ (dB)	$\|S_{31}\|$ (dB)	$\|S_{41}\|$ (dB)
Band I	Without stub	14.39	18.95	15.83	18.77
	With stub	30.26	21.47	19.42	21.04
Band II	Without stub	30.31	32.42	32.95	31.75
	With stub	30.82	38.98	30.16	38.69

From this table, we remark that using a stub improves the isolation. Therefore, it is clear that the isolation is better for the antenna with stub. Consequently, there is a lower mutual coupling between the four ports.

From all these results, we can conclude that high isolation was achieved using polarization diversity and inserting a stub in the ground plane.

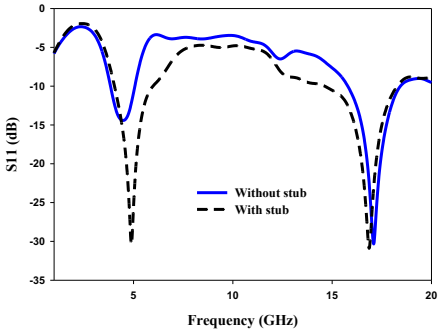

(a)

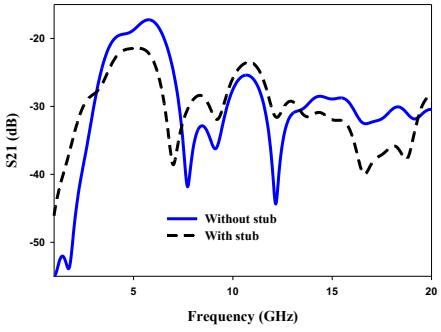

(b)

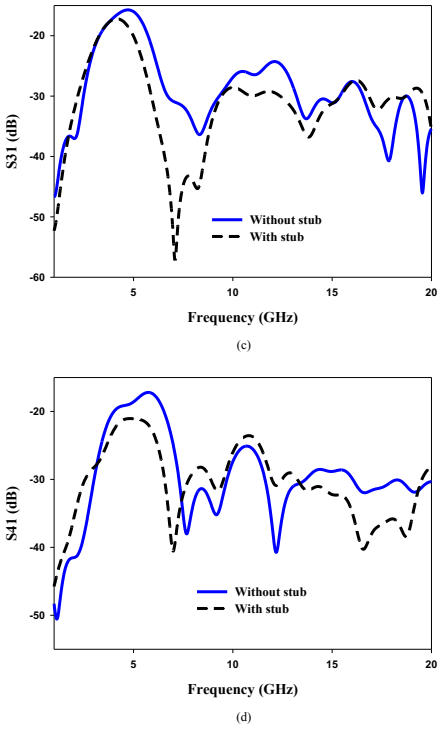

FIGURE 9. Simulated S-parameters of the proposed MIMO antenna without and with stub.

Finally, the simulated reflection and transmission coefficients of the proposed CPW dual-band MIMO antenna with optimal dimensions (Table 1) are illustrated in Fig. 10.

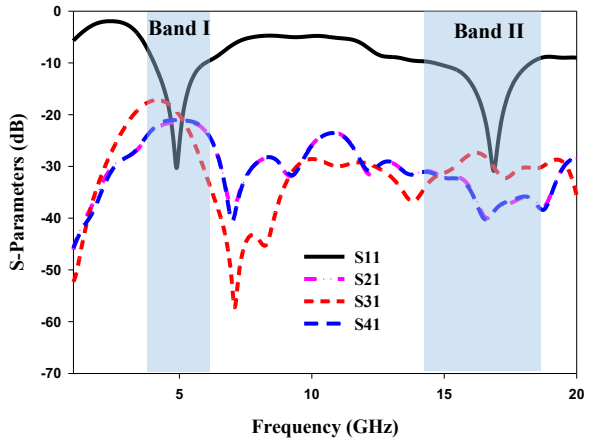

FIGURE 10. Simulated S-parameters of the proposed four-element CPW MIMO antenna.

The distribution of surface currents at 4.9 GHz and 16.9 GHz for the proposed CPW dual-band antenna will be described to confirm the decoupling between the antenna elements. Fig. 11 represents the simulated surface current distributions when port 1 is excited and the other ports are terminated at 50 Ω.

From Fig. 11 (a), it is clear that the current is mainly concentrated around the two slits etched on the radiating element; while it is focused around the I-shaped slot, as can be seen in Fig. 11 (b). Furthermore, the coupling current concentration between the MIMO antennas is negligible. Therefore, we can conclude that excellent isolation between the four antenna elements is ensured.

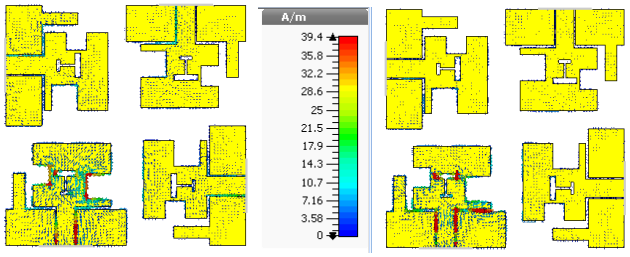

(a) fr=4.9 GHz (b) fr=16.9 GHz

FIGURE 11. Surface current distributions of the proposed MIMO antenna at: (a) 4.9 GHz and (b) 16.9 GHz.

III. FABRICATED ANTENNA AND MEASUREMENTS RESULTS

A. FABRICATED ANTENNAS

The proposed single and 4x4 CPW dual-band MIMO antennas are fabricated using a printed circuit board (PCB) milling machine: the LPKF Proto Mat E33. Then, the S parameters are measured using a Rohde and Schwarz ZVB 20 vector network analyzer (10 MHz - 20 GHz). The photographs of the fabricated prototype of single and MIMO antennas are illustrated in Fig. 12.

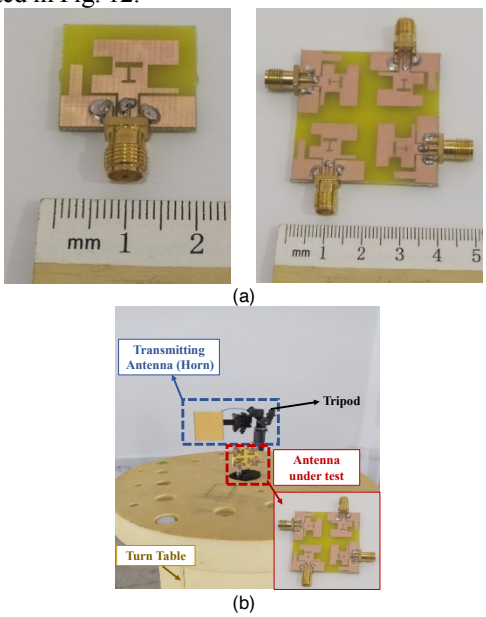

FIGURE 12. Photograph of fabricated prototypes single and MIMO antennas (a), measurement setup for the fabricated MIMO antenna (b).

B. S-PARAMETERS

The measured and simulated reflection coefficient of the proposed CPW single dual-band antenna are compared in Fig. 13. One can see an acceptable agreement between

measurement and simulation results. The impedance bandwidths (S_{11}<-10 dB) of the proposed MIMO antenna are [4.28-5.7 GHz] and [15-18.6 GHz] resonated at 4.89 GHz (lower-frequency band) with 41.31 dB and 16.8 GHz (upper-frequency band) with 52.1 dB, respectively.

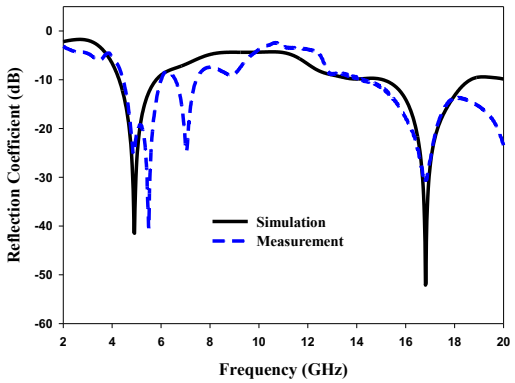

FIGURE 13. Measured and simulated S11 of the proposed single CPW dual-band antenna.

A comparison between measured and simulated S-parameters of the proposed CPW MIMO antenna is illustrated in Fig. 14. The detailed values of measured and simulated reflection and transmission coefficients at the lower and upper-frequency bands are summarized in Table 3. A close agreement between experimental and measurement results is observed. Additionally, the measured isolations are higher than 24 and 28 dB in both operating bands, indicating good MIMO performance.

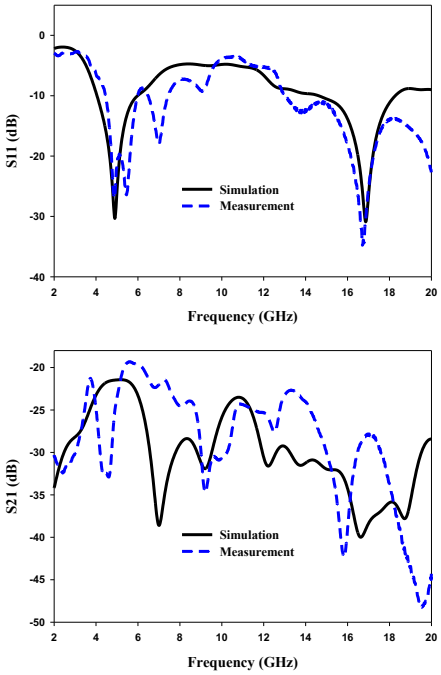

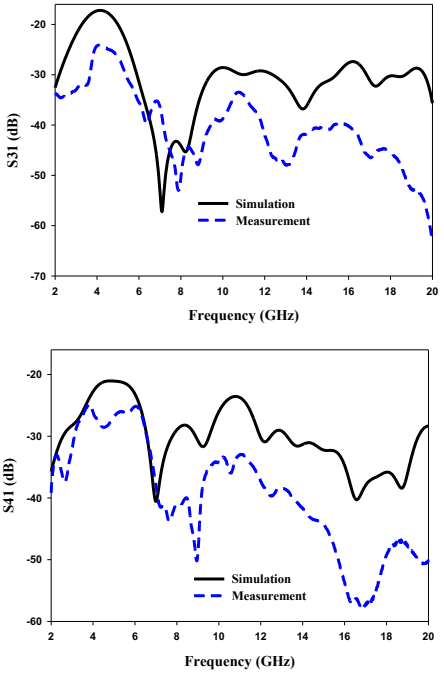

FIGURE 14. Measured and simulated S-parameters of the proposed CPW dual-band MIMO antenna.

TABLE III. Measured and simulated S-parameters of the proposed MIMO antenna

	Lower frequency band (Band I)		Upper frequency band (Band II)	
	Measured	Simulated	Measured	Simulated
fr (GHz)	4.86	4.87	16.7	16.9
$\|S_{11}\|$ (dB)	26.97	29.99	34.52	30.26
$\|S_{21}\|$ (dB)	24.23	21.46	28.29	39.06
$\|S_{31}\|$ (dB)	26.04	19.61	45.55	29.63
$\|S_{41}\|$ (dB)	27.19	21.05	57.76	38.92

C. PERFORMANCES OF MIMO ANTENNA

The objective of this section is to calculate and analyze several important parameters to evaluate a multiple-input, multiple-output antenna. They include envelope correlation coefficient "ECC", diversity gain "DG" and total active reflection coefficient "TARC" as well as efficiency and gain.

The Envelope Correlation Coefficient (ECC) is an important parameter that indicates the correlation between radiating elements. To calculate it, there are two approaches: the far-field radiation pattern [21] and the S parameters [17]. For good MIMO operation, this coefficient must be less than 0.5 [22].

The envelope correlation coefficient between antenna i and antenna j is calculated using complex radiation far-field and S-parameters by equations (1) and (2), respectively:

$$\rho_e(i,j) = \frac{\left| \oiint A_{ij}(\theta,\varphi) \sin\theta \, d\theta \, d\varphi \right|^2}{\oiint A_{ii}(\theta,\varphi) \sin\theta \, d\theta \, d\varphi \; . \; \oiint A_{jj}(\theta,\varphi) \sin\theta \, d\theta \, d\varphi} \quad (1)$$

Where:

$$A_{ii}(\theta,\varphi) = E_{\theta,i}(\theta,\varphi)\, E^{*}_{\theta,j}(\theta,\varphi) + E_{\varphi,i}(\theta,\varphi)\, E^{*}_{\varphi,j}(\theta,\varphi)$$

$E_{\theta,i}(\theta,\varphi)$ is the electric field radiated by the antenna element i.

$$\rho_e(i,j,N=4) = \frac{\left|\sum_{n=1}^{4} S^{*}_{in} S_{nj}\right|^2}{\left(1-\sum_{n=1}^{4}|S_{ni}|^2\right)\left(1-\sum_{n=1}^{4}|S_{nj}|^2\right)} \quad (2)$$

The diversity gain (DG) is related to the ECC, and they are connected by the following equation (3):

$$DG = 10\sqrt{1-|\rho|^2} \quad (3)$$

Where: $|\rho|^2 = \rho_e$

Fig. 15 represents the measured and simulated ECC and DG of the proposed CPW dual-band MIMO antenna. Note that the simulated ECC from the complex radiation far-field and S-parameters were obtained from CST, whereas the measured ECC is calculated from the S-parameters of the proposed MIMO antenna. From Fig. 15, it can be seen that the measured value of ECC (1,2) and ECC (1,3) are close to zero, while DG is about 10 at the lower and upper bands, respectively. It should be noted that all ECC values are below 0.5, which indicates good diversity performance of the proposed CPW dual-band MIMO antenna.

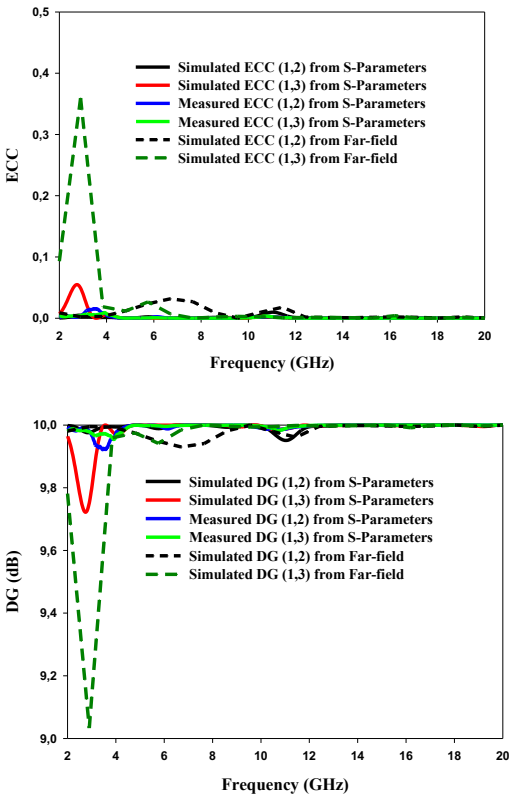

FIGURE 15. Measured and simulated ECC and DG of the proposed MIMO antenna.

The Total Active Reflection Coefficient is the square root of the sum of all reflected powers at the ports, divided by the sum of all incident powers at the ports of a 4-port antenna. TARC can be obtained directly from the scattering matrix by equation (4) [23]:

$$\Gamma = \frac{\sqrt{\sum_{i=1}^{4}|B_i|^2}}{\sqrt{\sum_{i=1}^{4}|A_i|^2}} \quad (4)$$

Where B_i and A_i are the reflected and incident signal, respectively.
The scattering matrix for the 4x4 antenna array can be written as follows:

$$\begin{pmatrix} B_1 \\ B_2 \\ B_3 \\ B_4 \end{pmatrix} = \begin{pmatrix} S_{11} & S_{12} & S_{13} & S_{14} \\ S_{21} & S_{22} & S_{23} & S_{24} \\ S_{31} & S_{32} & S_{33} & S_{34} \\ S_{41} & S_{42} & S_{43} & S_{44} \end{pmatrix} \begin{pmatrix} A_1 \\ A_2 \\ A_3 \\ A_4 \end{pmatrix} \quad (5)$$

From equations (4) and (5), the formula of TARC can be shown as follows [2]:

$$TARC = \sqrt{\frac{|(S_{ii}+S_{ij}e^{j\theta})|^2+|(S_{ji}+S_{jj}e^{j\theta})|^2}{4}} \quad (6)$$

Fig. 16 represents the measured and simulated TARC of the proposed MIMO antenna. As can be seen from this figure, TARC is better than -10 dB at the operating bands.

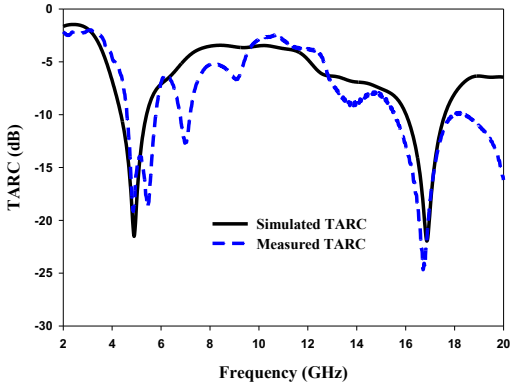

FIGURE 16. Measured and simulated TARC of the proposed MIMO antenna.

The proposed MIMO antenna's simulated radiation efficiency and realized gain are plotted in Fig. 17. The radiation efficiencies are 70% and 65% at lower and upper-frequency bands, respectively. The realized gain is 2.65 dB at the lower-frequency band and 4.36 dB at the upper-frequency band.

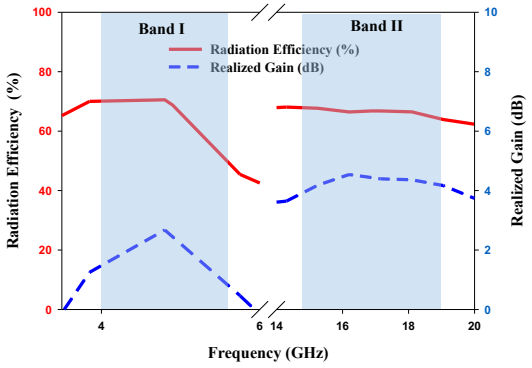

FIGURE 17. Radiation efficiency and realized gain of the proposed MIMO antenna.

D. RADIATION PATTERN

Fig. 18 presents the measured and simulated radiation pattern of the proposed CPW dual-band MIMO antenna in the E-plane and H-plane at 4.9 GHz and 16.9 GHz when port 1 is excited and other ports are terminated with a 50 Ω load. As shown in figure 18, there is a good agreement between the measurement and simulation results. It can be noted that in H-plane, the radiation pattern is purely omnidirectional (shape of "O"), whereas, in E-plane, the radiation pattern is bidirectional (shape of "8"), identical to the radiation pattern of a dipole antenna at the lower frequency and nearly omnidirectional at the upper frequency.

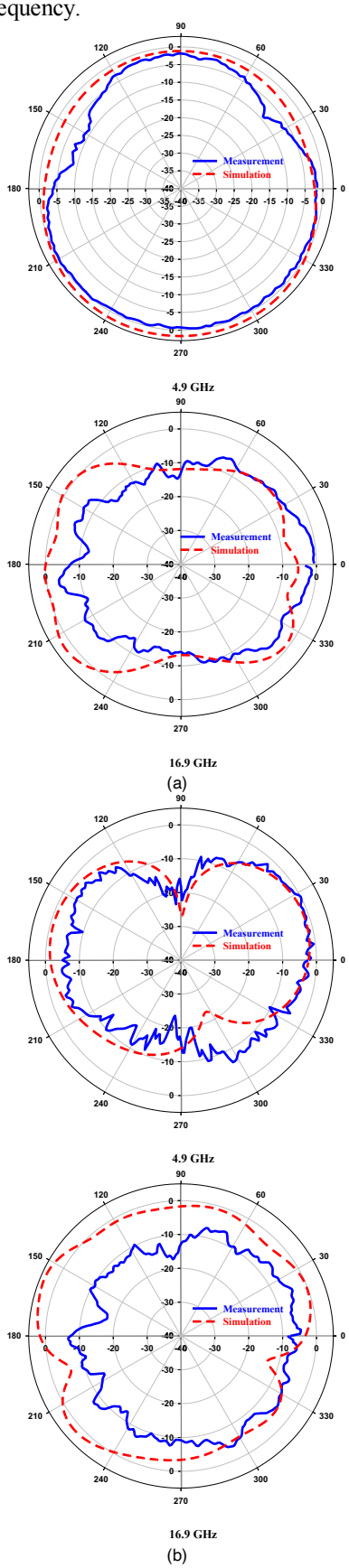

FIGURE 18. The proposed MIMO antenna's measured and simulated radiation pattern in: (a) H plan and (b) E plan.

E. PERFORMANCE COMPARISON

The comparison of performance regarding overall size, number of elements, bandwidth, isolation, ECC, and diversity gain between the proposed CPW dual-band 4x4 MIMO antenna and recently published articles is shown in Table 4.

Based on this table, our antenna has a very compact size, high isolation, and a low ECC compared to all listed references. In addition, the proposed antenna has a simple structure and wide bandwidth. Therefore, the suggested antenna is suitable for MIMO system applications and is a good candidate for 5G mobile and satellite communications.

TABLE IV. Performance comparisons of the proposed CPW dual-band 4x4 MIMO antenna with recently published works

Ref	N° elt	Size/ Substrate	Fr (GHz)	Bandwidth (GHz)	Isolation (dB)	ECC	DG (dB)
This Work	4	40x40 FR4	4.9 17	[4.05-5.97] [14.6-18.25]	27 30	0.0001 $2.34x10^{-7}$	9.999 10
[3]	2	54x27 FR4	4.9	[4.82-5]	23	0.002	_
[24]	4	120x65 FR4	3.5 4.8	[3.3-5]	18.8	0.018	_
[25]	4	50x50 FR4	3.4 4.9	[3.3-5.8]	20	0.01	_
[21]	4	150x73 FR4	3.5 4.9	[3.4-3.6] [4.8-5]	17.5 20	0.14 0.12	_
[26]	2	74x47.3 FR4	2.51 5.21	[2.46-2.7] [5.04-5.5]	30	0.01	_
[27]	4	130x74 FR4	3.5 4.9	[3.3-3.6] [4.8-5]	15 12	0.1	_
[28]	4	100x60 Rogers	3.46 17	_ [16.5-17.8]	10 15	0.04 0.02	_
[29]	2	72x36 FR4	2.4 4 6.1	[2.33-2.82] [3.68-4.31] [5.73-6.48]	20	0.007	_
[30]	4	50x50 FR4	5.2	[4.3-6.65]	20	0.004	9.9

IV. CONCLUSION

A novel dual-band four-element multiple input multiple output antenna is proposed in this work. The proposed antenna is designed and fabricated on an FR4 substrate; its overall dimension is 40x40x1.6 mm^3. The fundamental element antenna has a dual resonance at 4.9 GHz and 17 GHz. The impedance bandwidth ranges from 4.05 to 5.97 GHz and from 14.6 to 18.25 GHz for a reflection coefficient of less than -10 dB, covering 5G and satellite applications. The polarization diversity technique and adding stub in the ground plane achieved isolation between ports higher than 30 dB in both bands. The envelope correlation coefficient ECC is less than 0.0001, and the diversity gain is greater than 9.99 at the lower and upper bands. Furthermore, the radiation efficiency is 70% and 65% at the lower and upper-frequency bands, respectively. Realized gain of 2.61 dB is obtained at 4.9 GHz and 4.32 dB at 17 GHz. The simulated results are validated by the experimental ones and shown an acceptable agreement. In addition to these features, the suggested antenna has a simple structure and compact size. Therefore, the proposed MIMO antenna is suitable for 5G mobile and satellite communication networks.

REFERENCES

[1] M. Shuhrawardy, M. H. Miah Chowdhury, and R. Azim, "A Four-element Compact Wideband MIMO Antenna for 5G Applications," in 2nd International Conference on Electrical, Computer and Communication Engineering, (ECCE),Cox'sBazar, Bangladesh, 2019, pp. 1–5.

[2] P. Gupta, L. Malviya, and S. V. Charhate, "5G multi-element/port antenna design for wireless applications:a review," Int. J. Microw. Wirel. Technol., vol. 11, no. 9, pp. 918–938, 2019.

[3] Y. Liu, X. Yang, Y. Jia, and Y. J. Guo, "A Low Correlation and Mutual Coupling MIMO Antenna," IEEE Access, vol. 7, pp. 127384–127392, 2019.

[4] D. El Hadri, A. Zakriti, A. Zugari, M. El Ouahabi, and J. El Aoufi, "High Isolation and Ideal Correlation Using Spatial Diversity in a Compact MIMO Antenna for Fifth-Generation Applications," Int. J. Antennas Propag., vol. 2020, pp. 1–10, 2020.

[5] L. Ming-Yang, X. Zi-Qiang, B. Yong-Ling, S. Chow-Yen-Desmond, and Y. Zhe-Feng, "Eight-port orthogonally dual-polarised MIMO antennas using loop structures for 5G smartphone," IET Microwaves, Antennas Propag., vol. 11, no. 12, pp. 1810–1816, 2017.

[6] M. Khalid et al., "4-port MIMO antenna with defected ground structure for 5G millimeter wave applications," Electronics, vol. 9, no. 1, pp. 1–13, 2020.

[7] R. Mathur and S. Dwari, "Compact 4-Port UWB-MIMO slot antenna with dual polarization and low correlation for spatial diversity application," Frequenz, vol. 72, no. 11–12, pp. 503–509, 2018.

[8] X. Shi, M. Zhang, S. Xu, D. Liu, H. Wen, and J. Wang, "Dual-band 8-element MIMO antenna with short neutral line for 5G mobile handset," in 11th European Conference on Antennas and Propagation (EUCAP), 19-24 March 2017, Paris, France, pp. 3140–3142.

[9] M. Abdullah, Y. L. Ban, K. Kang, M. Y. Li, and M. Amin, "Eight-element antenna array at 3.5GHz for MIMO wireless application," Prog. Electromagn. Res. C, vol. 78, pp. 209–216, 2017.

[10] M. Daghari, C. Abdelhamid, H. Sakli, and K. Nafkha, "High isolation with neutralization technique for 5g-mimo elliptical multi-antennas," in Smart Innovation, Systems and Technologies, 2020, vol. 147, pp. 124–133.

[11] R. N. Tiwari, P. Singh, B. K. Kanaujia, and K. Srivastava, "Neutralization technique based two and four port high isolation MIMO antennas for UWB communication," AEU - Int. J. Electron. Commun., vol. 110, pp. 1–10, 2019.

[12] T. Azari-Nasab, C. H. Ghobadi, B. Azarm, and M. Majidzadeh, "Triple-band operation achievement via multi-input multi-output antenna for wireless communication system applications," Int. J. Microw. Wirel. Technol., vol. 12, no. 3, pp. 259–266, 2020.

[13] M. Farahani, J. Pourahmadazar, M. Akbari, M. Nedil, A. R. Sebak, and T. A. Denidni, "Mutual Coupling Reduction in Millimeter-Wave MIMO Antenna Array Using a Metamaterial Polarization-Rotator Wall," IEEE Antennas Wirel. Propag. Lett., vol. 16, no. c, pp. 2324–2327, 2017.

[14] A. Dkiouak, A. Zakriti, M. El Ouahabi, N. A. Touhami, and A. Mchbal, "Design of a four-element MIMO antenna with low mutual coupling in a small size for satellite applications," Prog. Electromagn. Res. M, vol. 85, no. July, pp. 95–104, 2019.

[15] Z. Xu, Q. Zhang, and L. Guo, "A compact 5G decoupling MIMO antenna based on split-ring resonators," Int. J. Antennas Propag., vol. 2019, pp. 1–10, 2019.

[16] M. El Ouahabi, A. Zakriti, M. Essaaidi, A. Dkiouak, and H. Elftouh, "A miniaturized dual-band MIMO antenna with low mutual coupling for wireless applications," Prog. Electromagn. Res. C, vol. 93, no. May, pp. 93–101, 2019.

[17] L. Malviya, R. K. Panigrahi, and M. V. Kartikeyan, "MIMO antennas with diversity and mutual coupling reduction techniques: A review," Int. J. Microw. Wirel. Technol., vol. 9, no. 8, pp. 1763–1780, 2017.

[18] H. Al-Saif, M. Usman, M. T. Chughtai, and J. Nasir, "Compact Ultra-Wide Band MIMO Antenna System for Lower 5G Bands," Wirel. Commun. Mob. Comput., vol. 2018, pp. 1–6, 2018.

[19] Q. Cai, Y. Li, X. Zhang, and W. Shen, "Wideband MIMO Antenna Array Covering 3.3-7.1 GHz for 5G Metal-Rimmed Smartphone Applications," IEEE Access, vol. 7, pp. 142070–142084, 2019.
[20] A. Kumar and M. Gupta, "A review on activities of fifth generation mobile communication system," Alexandria Eng. J., vol. 57, no. 2, pp. 1125–1135, 2018.
[21] Z. Ren and A. Zhao, "Dual-Band MIMO Antenna with Compact Self-Decoupled Antenna Pairs for 5G Mobile Applications," IEEE Access, vol. 7, pp. 82288–82296, 2019.
[22] Y. L. Ban, C. Li, C. Y. D. Sim, G. Wu, and K. L. Wong, "4G/5G Multiple Antennas for Future Multi-Mode Smartphone Applications," IEEE Access, vol. 4, pp. 2981–2988, 2016.
[23] F. Wang, Z. Duan, X. Wang, Q. Zhou, and Y. Gong, "High isolation millimeter-wave wideband MIMO antenna for 5G communication," Int. J. Antennas Propag., vol. 2019, pp. 1–12, 2019.
[24] A. Biswas and V. R. Gupta, "Design and Development of Low Profile MIMO Antenna for 5G New Radio Smartphone Applications," Wirel. Pers. Commun., vol. 111, pp. 1695–1706, 2020.
[25] J. Su, Z. Dai, J. Du, J. Yu, Z. Chen, and Z. Li, "A Compact Dual-band MIMO Antenna for 5G Mobile Communications," ACES J., vol. 34, no. 11, pp. 1731–1738, 2019.
[26] P. Liu, D. Sun, P. Wang, and P. Gao, "Design of a Dual-Band MIMO Antenna with High Isolation for WLAN Applications," Prog. Electromagn. Res. Lett., vol. 74, pp. 23–30, 2018.
[27] W. Zhang, Z. Weng, and L. Wang, "Design of a Dual-band MIMO Antenna for 5G Smartphone Application," in International Workshop on Antenna Technology (iWAT), 5-7 March 2018, Nanjing, China, pp. 1–3.
[28] M. S. Sharawi, M. Ikram, and A. Shamim, "A Two Concentric Slot Loop Based Connected Array MIMO Antenna System for 4G/5G Terminals," IEEE Trans. Antennas Propag., vol. 65, no. 12, pp. 6679–6686, 2017.
[29] P. Rezai, A. Valizade, J. Nourinia, M. Solimanejad, F. Alizadeh, and B. Mohammadi, "Design of A Triple-Band Compact Microstrip Monopole Antenna Using Multiple Bent-Lines with Low Correlation for MIMO Applications," in 24th Iranian Conference on Electrical Engineering (ICEE),Shiraz,Iran, 2016, pp. 768–771.
[30] A. W. Mohammad Saadh et al., "A compact four-element MIMO antenna for WLAN/WiMAX/satellite applications," Int. J. Commun. Syst., vol. 33, no. 14, pp. 1–17, 2020.